Febrile seizure unleashes spreading depolarizations in Scn1a deficient mice

Isamu Aiba*, Yao Ning, Jeffrey L Noebels

Department of Neurology, Baylor College of Medicine, One Baylor Plaza, Houston TX 77030

Abstract

Objective: Spreading depolarization (SD) is a massive wave of cellular depolarization that slowly migrates across brain gray matter. SD is frequently generated following brain injury and is associated with various acute and chronic neurological deficits. Here we report that spontaneous cortical SD waves are a common EEG abnormality in the Scn1a deficient mouse model ($Scn1a^{+/R1407X}$).

Method: Chronic DC-band EEG recording detected SDs, seizures, and seizure-SD complexes during prolonged monitoring in awake adult $Scn1a^{+/R1407X}$ mice. The effect of hyperthermic seizure and memantine was tested.

Results: The spontaneous incidence of events is low and varied among animals, but SDs outnumber seizures. SD waves almost always spread unilaterally from parietal to frontal cortex. On average, spontaneous SD frequency robustly increased by 4.2-fold following a single hyperthermia-evoked seizure, persisting for days to a week without altering the kinetics of individual events. Combined video image and electromyogram analyses revealed that a single interictal SD is associated with prodromal motor activation followed by minutes-lasting immobility upon invasion of frontal cortex. Similar behavioral sequelae also appeared during postictal SD. Memantine treatment was effective in preventing SD exacerbation when given before and after the hyperthermic seizure, suggesting chronic activation of NMDA-receptor contributed to the prolonged SD aftermath.

Interpretation: Our results reveal that cortical SD is a prominent electro-behavioral phenotype in this Scn1a deficient mouse model, and SD frequency is robustly sensitive to hyperthermic seizure induced mechanisms likely involving excess NMDAR signaling. The high susceptibility to SD may contribute to co-morbid pathophysiology in developmental epileptic encephalopathy.

Introduction

Spreading depolarization (SD) is a massive self-regenerative wave of minutes lasting near-complete cellular depolarization slowly propagating across brain gray matter [1,2]. The profound cellular depolarization leaves prolonged hypoperfusion and depression of spontaneous neuronal activity, contributing to transient dysfunction in the affected brain area. SD is frequently generated in patients after brain injuries and is associated with acute and chronic neurological deficits. SD is also associated with visual and motor deficits in some genetic migraine with aura syndromes [3], and experimental studies suggest that repetitively provoked SD can produce migraine comorbidities such as photosensitivity, hyperalgesia, and anxiety [4,5]. There is a growing interest in understanding SD generation mechanisms and therapeutic interventions.

Due to their excitatory nature, SD events are detected in association with seizures or epileptic discharges in both experimental and clinical settings [6,7]. Such “peri-ictal” SD events have been considered as a candidate mechanism contributing to epilepsy comorbidities such as peri-ictal migraine headache and immobility [8].

However, understanding of SD incidence in epilepsy is extremely limited. Using chronic DC-band EEG recording in awake freely behaving mice, we directly demonstrated that SD is spontaneously generated not only in the peri-ictal, but also in the interictal phase of awake mice bearing epileptogenic Kcnq2 and Kcna1 potassium channel mutations [7]. On the other hand, it remains unknown whether these spontaneously generated cortical SD waves might contribute to neurological deficits arising in developmental epilepsy syndromes.

Mutations in sodium channel genes are a common cause of developmental epileptic encephalopathy (DEE), and both gain- and loss of function mutations in the *SCN1A*/Nav1.1 gene are identified across a range of DEE phenotypes. Scn1a/Nav1.1 channels are widely expressed in both human and rodent neocortices [9–11], however, their dysfunction preferentially impacts specific neuronal populations, such as fast-spiking inhibitory neurons [12,13]. Gain-of-function SCNA1 mutations have been identified in rare genetic hemiplegic migraine type-III patients where increased excitability of interneurons may enhance extracellular K^+ elevation and contribute to SD susceptibility [14]. The more common *SCN1A* loss-of-function mutations are associated with epileptic encephalopathies (e.g. Dravet syndrome) with a range of severity depending on the type of mutation [15]. In these cases, reduced inhibitory neuron excitability results in network disinhibition and the emergence of hyperexcitable neuronal circuitry [12], and febrile seizures trigger and exacerbate epileptic encephalopathy [16]. It is not known whether febrile seizure in this channelopathy model affects SD susceptibility and neurobehavioral deficits.

In this study, we identified the spontaneous SD incidence in the Scn1a deficient $Scn1a^{+/R1407X}$ (hereafter $Scn1a^{+/RX}$) mice using DC-band cortical EEG recording, and spontaneous SD can be profoundly increased by a single hyperthermic seizure. The flurry of SD events persists for days or a week and can be inhibited by administration of memantine targeting NMDAR activation during and after the hyperthermic seizure. We also established that these SD events are not purely electrographic, but are associated with distinct motor behavior patterns. Together, our study revealed a new aspect of Scn1a deficient epileptic encephalopathy and suggest SD as a potential contributor to co-morbidity mechanisms in Dravet Syndrome.

Materials and Methods

Animals

All animal experiments were conducted under the guide of AAALAC and approved by IACUC of Baylor College of Medicine. $Scn1a^{R1407X/+}$ mice [13] were backcrossed with heterozygote flox-tdtomato line (100% C57Bl6 background, Ai9, Jackson Laboratory #007909) and maintained on 75-82.8% C57Bl6 and 25-12.5% SV129 background. The flox-tdtomato allele is inactive in the absence of Cre recombinase, and was used as a post-hoc label to blind the experimenter to genotype or treatment. Littermate wild-type (WT) mice were used as control. During the breeding and chronic recording study, the mice have ad-lib access to mouse chow (5V5M, PicoLab) and drinking water in rooms maintained at 20-24°C and 40-70% humidity with a 12-hour light-dark cycle.

Surgery

Mice were injected with meloxicam (5 mg/kg, s.c.) as a presurgical analgesic, and anesthetized with isoflurane (3.0% induction, 1.5-2.5% maintenance) while body temperature was maintained with a heating mat. The scalp hair is depilated and the skin cleansed with betadine and 70% ethanol 3 times. After injection of local

anesthetics (1% lidocaine, 1% bupivacaine mixture), a midline skin incision is made to expose the skull surface, connective tissues are removed with cotton swabs. Cranial burr holes (~1 mm diameter) were made 0.5 mm anterior/2.0 mm lateral and 2.5 mm posterior/2.5 mm lateral from the bregma and two burr holes in the occipital bone; the position occasionally required adjustment by ~0.5 mm when major blood vessels were present. In each burr hole, a drop of dexamethasone (10 mg/ml) was topically applied to ameliorate the inflammatory tissue damage. Teflon-insulated silver wires (36-G or ~0.13 mm diameter) were carefully positioned over the cortical surface and a pair of wires were inserted under the neck muscles for electromyogram (EMG) recording. After implantation, the wires and connector are cemented to the skull with metabond. Mice received meloxicam (5 mg/kg) for 3 postoperative days. In order to minimize postsurgical effect, EEG recordings were initiated at least 7 days after the implant.

Video EEG recording of awake mice

EEG recordings were conducted in an IACUC-approved satellite room (20-22°C, 40% humidity, 12-hour light-dark cycle). Each mouse was connected to a fine EEG tether wire and housed in a 30 x 15 cm home cage with freely available water and food. EEG activity was acquired using a Bioamp DC amplifier and digitized by the LabChart system (ADI) while the monitoring unit was continuously recorded using an IR-light equipped CMOS camera at 2Hz. The EEG signals were analyzed using LabChart (ADI) and Clampfit 10 software (Molecular devices). All raw EEG traces were visually inspected for seizure and SD incidence and were manually quantified based on their characteristic EEG forms. Postictal generalized EEG suppression (PGES) was defined as the complete suppression of EEG amplitude immediately after seizure termination and the duration was determined based on the total EEG power (total EEG power <0.01 mV^2, see **Figure 3A**). The video image was analyzed using Bonsai and R software. Some video images were excluded from the analysis because the mouse position could not be accurately resolved.

Induction of hyperthermic seizure

A hyperthermic seizure was then induced at 11-12 a.m. in a glass-walled chamber using a combined heating lamp and cooling mat. Hyperthermia was induced using a heating lamp while cortical EEG and body temperature were continuously monitored. As soon as a seizure was detected, the mouse was placed on an iced mat to cool the body to 37°C. The mice were then returned to the recording cage and EEG monitoring was continued for 10 days. Some mice were recorded for an extended period to sample seizures for EMG signals analysis.

Drug

Memantine was purchased from Tocris and dissolved in saline on the day of the experiment and administered intraperitoneally.

Study design and statistics

EEG recording studies included both male and female Scn1a Het and WT in each cohort. Two to four mice were simultaneously recorded in each cohort of the study. Because some littermate mutant mice died during the study, we added several Scn1a mutant mice, resulting in an unequal number of mice by sex.

Statistics were calculated by R software and GraphPad prism. In cases where sample distribution was skewed and sample numbers were different, we chose non-parametric statistical methods, aligned rank transformation ANOVA for multiple comparisons [17], and Mann-Whitney U-test for two sample comparisons. Otherwise, statistics were computed using standard parametric tests. The test used for each study is described in the figure legends. Unless specifically mentioned, data are presented as mean ± S.D.

Results

Chronic monitoring of spontaneous cortical SD and seizures in Scn1a deficient mice

We characterized SD incidence of Scn1a deficient (Scn1a$^{+/RX}$) and WT mice using a DC-band chronic EEG recording method reported in our previous study [7]. In the study cohorts, we recorded a total of seventeen Scn1a$^{+/RX}$ (7 males, 10 females) and eleven littermate WT mice (5 males and 6 females). Recordings started at the age of P40-96. After 7 days of baseline recordings, mice were subjected to a hyperthermic seizure (detail described later) and the effect was monitored for 10 days.

The results are summarized in **Figure 1**. We detected both spontaneous SD, seizures, and seizure with postictal SD (hereafter "seizure+SD") in which an SD emerged shortly following a seizure (**Figure 1A-C**). During the study, seven Scn1a$^{+/RX}$ mice were lost due to sudden death or postictal moribund condition (**Figure 1D**). While the incidence of seizure and SD was relatively rare (total events: 0.57 ± 0.35 /day), SD was more commonly detected than seizures in baseline in most mice (**Figure 1E-F**). No seizures or SD were detected in WT mice during the baseline or post-hyperthermia periods (**Figure 1D**).

After baseline recording, mice were subjected to a hyperthermic seizure (details later) and its effect was continuously monitored for >7 days. Starting one day after post-hyperthermic seizure, SD frequency clearly increased in Scn1a$^{+/RX}$ mutant (**Figure 1D&E**), even in two mice that had not shown any seizure or SD during baseline recording. This upsurge in SD frequency could last for multiple days and up to a week, making SD the dominant EEG event (**Figure 1F**). Statistical analyses detected significant increases in the frequencies of spontaneous SD (4.2-fold) and total events (3.3-fold) following the hyperthermic seizure (**Figure 1G**). In the two exceptional "seizure-only" mice that did not show SD during baseline nor during the hyperthermic seizure, seizure frequency actually decreased after hyperthermic seizure. These results suggest prior disease status could significantly affect the consequence of hyperthermic seizure. However, because of the rare chance to encounter them, we could not specifically analyze more of these mice. There were no changes in seizure/SD frequency in the control mice without a hyperthermic seizure.

There was a weak diurnal trend in the seizure and SD frequencies **(Figure 1H)**. Seizure/SD incidence was higher during the interval between 18-20 h, corresponding to the transition to the dark phase. A similar peak was detected in the SUDEP rate in the same Scn1a deficient mouse model [18], confirming the presence of circadian vulnerability.

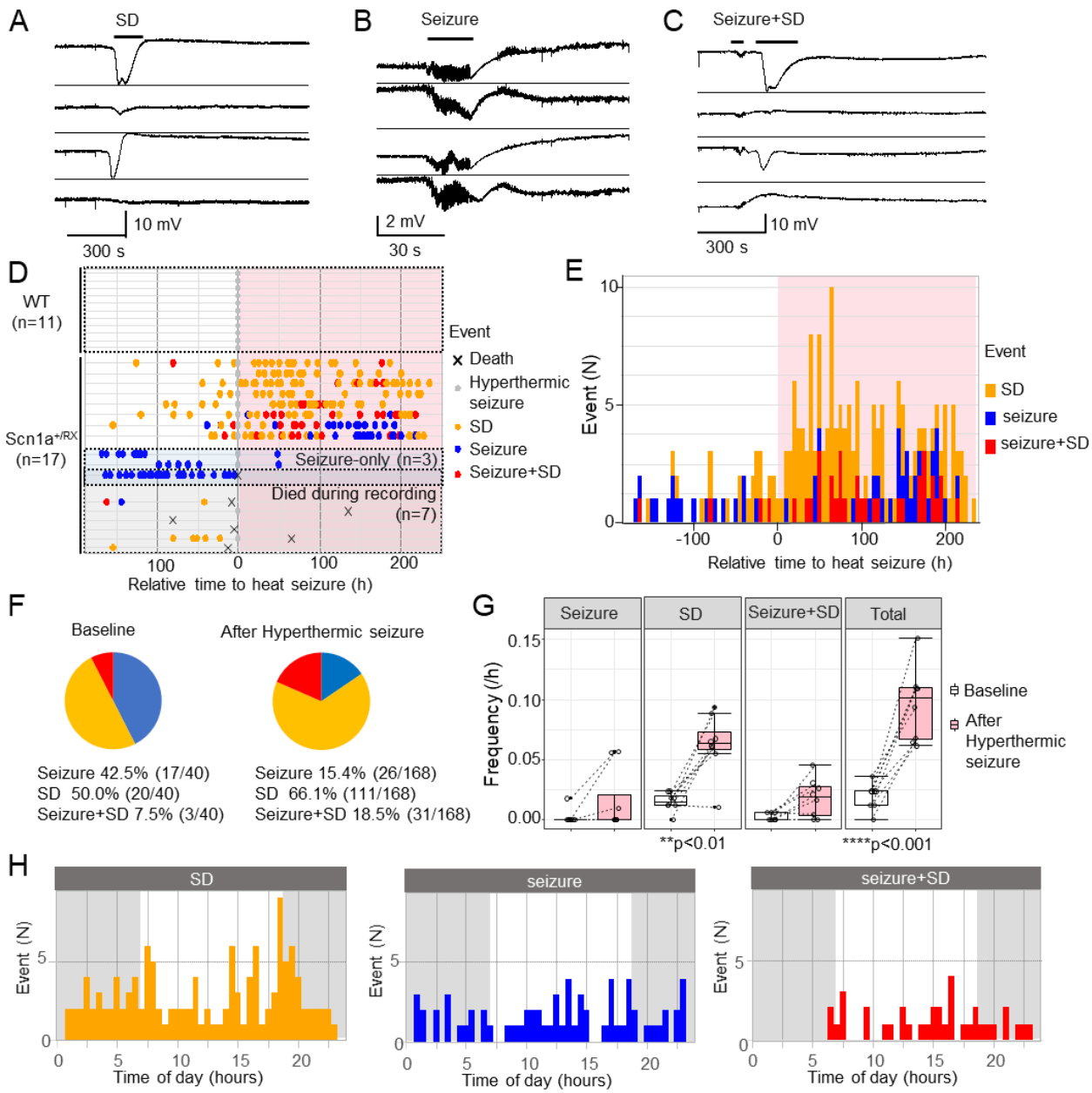

Figure 1 Seizure and SD phenotype of Scn1a$^{+/RX}$ mice before and after a hyperthermic seizure. **A-C** representative traces of SD, seizure, and seizure+SD complex. **D-E** hyperthermic seizure robustly increased SD and seizure incidence. **D.** Raster plots of seizure and SD incidence in WT and Scn1a$^{+/RX}$ mice. There were three mice that exclusively had seizures ("seizure-only"). **E.** The same Scn1a$^{+/RX}$ even data is presented in a cumulative histogram. **F.** Proportion of seizure, SD, and seizure+SD during baseline and after hyperthermic seizure in the Scn1a$^{+/RX}$ mice which survived the recording period, excluding the "seizure-only" mice. **G.** Quantification of event frequencies. Frequencies of SD and total events were increased after a hyperthermic seizure. "Seizure-only" mice were excluded from this analysis. Two–way ANOVA and post hoc Tukey test. **H.** Chronological analysis of SD, seizure, and seizure SD events

High SD susceptibility during the hyperthermic seizure in Scn1a$^{+/RX}$ mice

In addition to spontaneous events, SD was also prominent during hyperthermic seizure. During heat exposure, Scn1a$^{+/RX}$ mice showed cortical spikes and significant drooling as the body core temperature approaches 40°C. The seizure onset of Scn1a$^{+/RX}$ always coincided with a vocalization, behaviorally associated with tremor in a hunched posture, and electrographically detected as a train of ictal spiking which may result within less than 1 minute in a coupled SD (**Figure 2A**). SD was detected in 82% (10/13) of the Scn1a$^{+/RX}$ mice during hyperthermic seizure and was usually associated with a loss of voluntary movement except for occasional myoclonic movement. It is noted that the three mice without SD during hyperthermic seizure were "seizure-only" mice, of which one died shortly after the hyperthermic seizure. In WT mice, SD was less common in hyperthermic seizures and detected in 27% (3/11, p=0.037 vs Het, Fisher's exact test, **Figure 2B&C**). Consistent with earlier studies [19], Scn1a deficient mice showed a lower temperature threshold for seizure compared to WT (WT: 43.0 ± 1.0°C, n=11, Scn1a$^{+/RX}$: 41.7 ± 0.7°C, n=12, p=0.007, Mann-Whitney test **Figure 2D**).

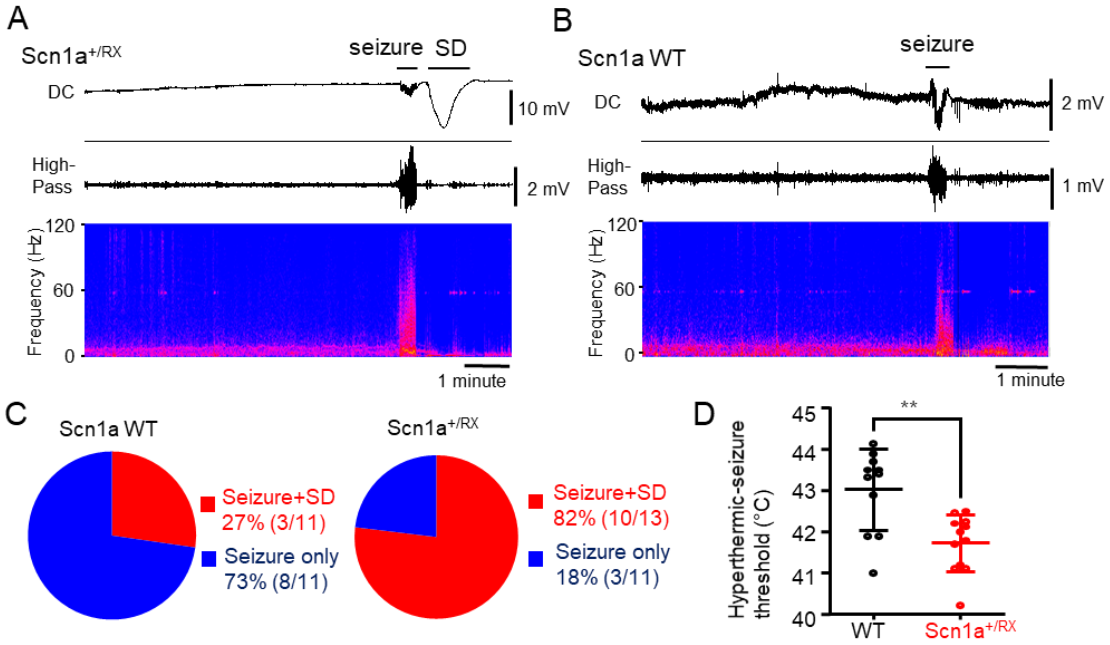

Figure 2 SD generation during hyperthermic seizures in Scn1a$^{+/RX}$ mice. Hyperthermic seizures were induced using a heating lamp. **A-C** 82% (10/13) of Scn1a$^{+/RX}$ mice developed SD following seizure (**A**), while it was less common in WT mice 27% (3/11, **B**). Traces: *top* DC, *middle* high pass (>1Hz), and *bottom* power spectrum of EEG (anterior electrode). **D.** Consistent with previous studies, Scn1a$^{+/RX}$ mice showed a lowered thermal threshold for seizure. p=0.007, Mann-Whitney U-test

Hyperthermic seizure did not modulate the kinetics of individual seizure and SD

In this study cohort, we detected a total of 160 SDs, 95 seizures, and 43 seizure+SD complexes. Regardless of the presence or absence of a preceding seizure, almost all SDs were detected first with the posterior electrode (isolated SD: 99% (159/160), seizure+SD: 98% (42/43)). These characteristics imply the presence of an SD susceptible region in the posterior cortex in Scn1a$^{+/RX}$ mice (see Discussion). While all seizures were detected as bilaterally generalized events, SDs were always unilateral.

Postictal generalized EEG suppression (PGES) is a simultaneous silencing of EEG activity across all electrodes immediately following a seizure, and the presence and duration often correlate with the clinical severity of postictal deficits [20]. In 47% (20/43) of seizure+SD complexes, we detected PGES lasting for 13.9 ± 5.0 seconds (**Figure 3A, B**). The period PGES could be clearly distinguished from a subsequent depression of EEG following SD. Neither PGES incidence nor duration was different after a seizure without postictal SD or a seizure with postictal SD (**Figure 3C-F**). Thus PGES in this mouse model is a separable process that did not seem to predict or correlate with postictal SD incidence.

Based on the increased spontaneous SD event frequency shown in **Figure 1D**, hyperthermic seizure was expected to facilitate the postictal SD generation by shortening the time to onset. However, the latency to postictal SD was significantly prolonged after hyperthermic seizure (**Figure 3D**). Hyperthermic seizure did not alter the kinetics of individual events, thus no differences were detected in the SD durations (baseline: 75.2 ± 24.7 s, n=39, after hyperthermic seizure: 72.1 ± 21.2 s, n=121, p=0.70), SD amplitudes (baseline: 9.4 ± 2.4 mV, n=39, after hyperthermic seizure: 8.9 ± 2.4 mV, n=121, p=0.18), seizure durations (baseline: 42.9 ± 13.3 s, n=44, after hyperthermic seizure: 41.9 ± 12.9 s, n=51, p=0.63), or seizure amplitudes (baseline: 2.3 ± 0.70 mV, n=44, after hyperthermic seizure: 2.5 ± 0.80 mV, n=51, p=0.46). Overall, the effect of hyperthermic seizure seems to be restricted to event generation pattern (event frequency, latency of postictal SD onset), and is without effect on the individual event severity.

The kinetics of SD and seizure activities detected in seizure+SD complexes differ from those detected individually. The duration of SD in seizure+SD complex was significantly shorter than those detected without a preceding seizure (duration: isolated SD 72.9 ± 21.8 s vs SD in "seizure+SD" 61.3 ± 22.6 s, p<0.0001, **Figure 3A**), and similarly, seizure duration is also shorter when detected in seizure+SD complex (duration: isolated seizure 41.5 ± 13.5 s vs seizure in seizure+SD 28.6 ± 9.6 s, p<0.0001, **Figure 3G**). On the other hand, the peak amplitudes of negative DC offset during SD and seizure were unchanged (**Figure 3B&3D**).

These analyses highlight the qualitative differences between seizure and SD components in a seizure+SD complex compared to those detected individually. The shorter seizure duration in seizure+SD complex suggests that the postical emergence of SD is somehow already determined once when the preceding seizure is generated, and thus isolated seizure and seizure+SD complexes might be independently regulated events.

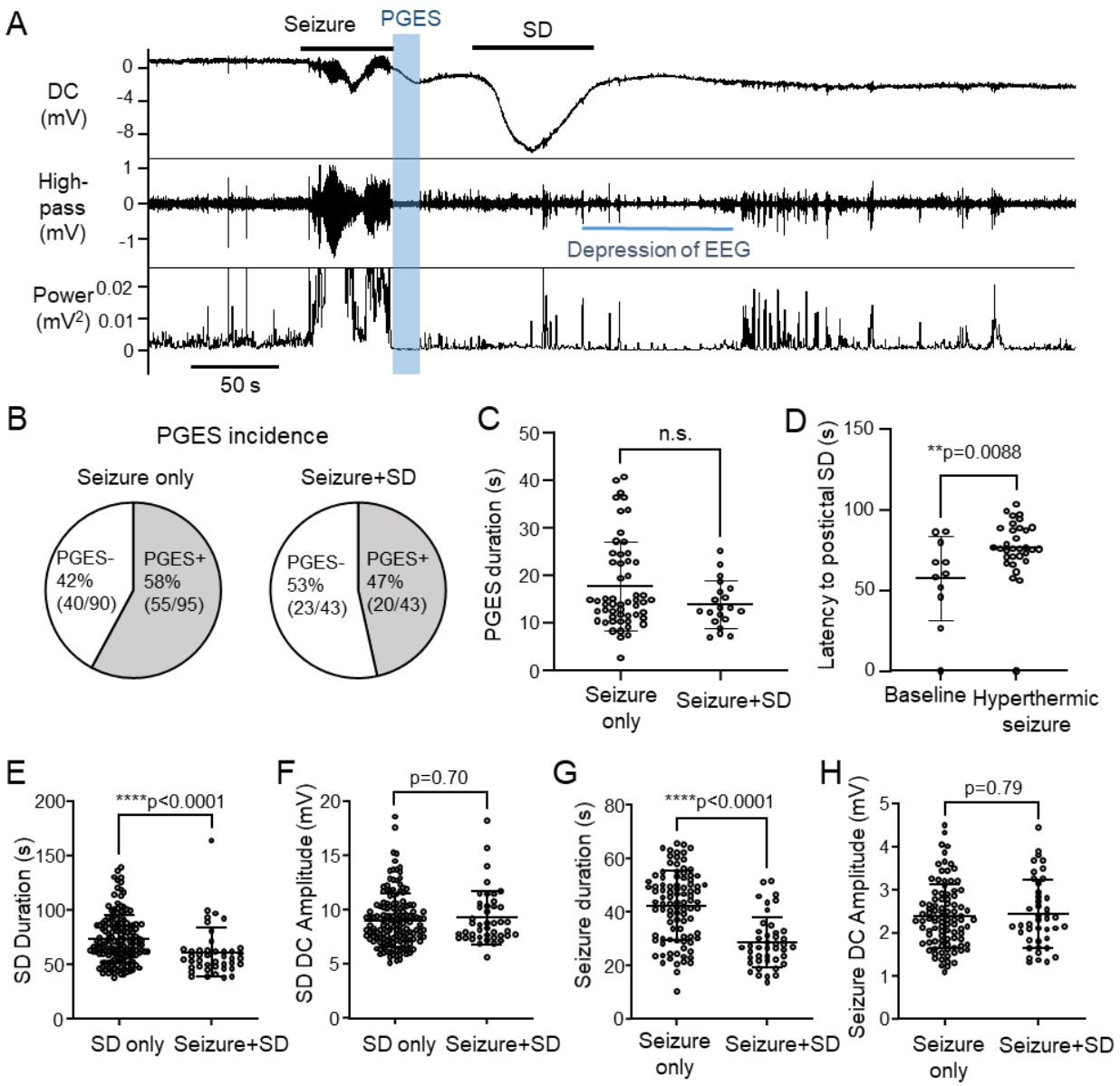

Figure 3 Electrophysiological characteristics of PGES and postictal SD. **A.** representative trace showing the temporal sequence of PGES (depressed EEG amplitude, blue window) and postictal SD generation. *Top*: DC, *Middle*: high pass (> 1Hz), *bottom*: EEG converted into power. The PGES incidence (**B**) and duration (**C**) were similar in seizure without postictal SD and seizure with post-ictal SD. **D.** The latency to SD after seizure termination is significantly prolonged after a hyperthermic seizure. **E-H** Comparison of seizure/SD kinetics between those in isolated events and those in the seizure+SD complex. The duration of SD in the seizure+SD complex is shorter than the duration of SD detected alone (**E**), while **t**he DC amplitudes were not different (**F**). Similarly, the duration of seizure in the seizure+SD complex is shorter than the duration of seizure that appeared without SD (**G**), while the DC amplitudes were not different (**H**). Statistics were computed by Mann-Whitney U-test

Memantine administration prevents the prolonged aftermath of a hyperthermic seizure

We examined whether pharmacological inhibition using the NMDAR antagonist memantine might attenuate the depolarizing aftermath of a hyperthermic seizure, since NMDAR activation has been implicated in a model of febrile seizure induced epileptogenesis [21]. Memantine is an FDA-approved NMDAR antagonist, and its rapid absorption and relatively short half-life in mouse brain (~4 hours [22]) proved useful in analyzing the hyperthermic seizure induced SD exacerbation. In this study, we chose 10 mg/kg (i.p.), a dosage that inhibits an NMDAR-dependent synaptic plasticity mechanism *in vivo* [23], and different administration patterns to investigate critical time windows; a pre-treatment (30-60 minutes before the febrile seizure), post-treatment (6 and 16 hours after febrile seizure induction), and a combined pre/post-treatment. The drug effect was evaluated by comparing the frequency of total events before and after the hyperthermic seizure induction.

The control group receiving saline before febrile seizure showed a robust increase in the total event (**Figure 4A**, p=0.0003). Compared with the initial cohort shown in **Figure 1**, more mice developed seizures following initial surges of SD. Significant increases in total events were seen in the pre-treatment (**Figure 4B**, p=0.012) or post-treatment groups (**Figure 4C**, p=0.048), while analysis of individual mice found that in two mice, the event number decreased in the post-treatment group. The hyperthermic-seizure induced increase in event frequency was inhibited in the memantine pre/post-treatment group (**Figure 4D**, p=0.25). Based on the half-life of memantine *in vivo*, these results collectively suggest that the hyperthermic seizure induced exacerbation of depolarizing phenotype NMDAR activation not only during but also ~16 hours after hyperthermic seizure. It is noteworthy that some mice in the prolonged memantine administration group showed recurrent seizures, which is likely related to the paradoxical hyperexcitation induced by memantine (see Discussion).

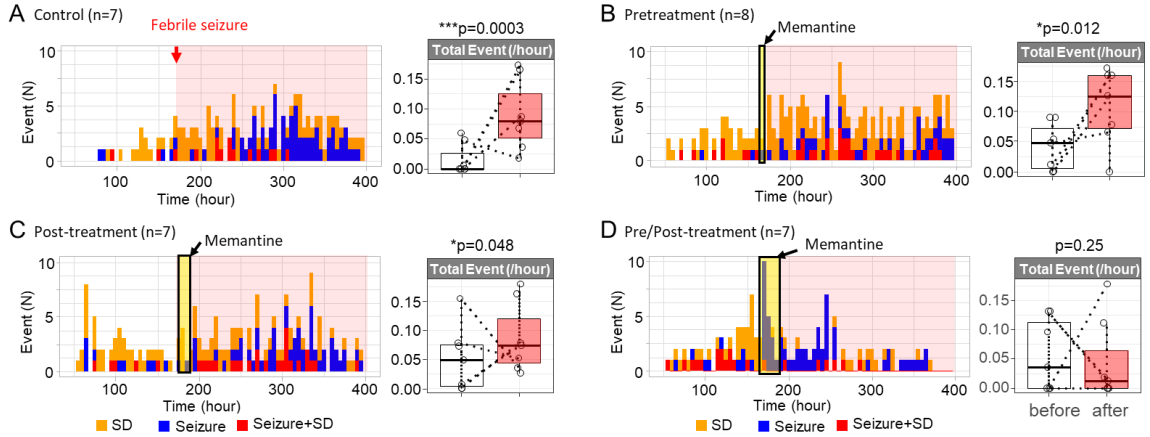

Figure 4 Prolonged memantine administration inhibits the hyperthermic seizure induced exacerbation of depolarizing events in Scn1a$^{+/RX}$ mice. Cumulative histograms show the incidence SD (orange), seizure (blue), and seizure+SD complexes (red) before and after hyperthermic seizure. Box-plots show total event frequency (total events per hour) during baseline (white) and after hyperthermic seizure (red). **A.** pattern of events in saline pretreated control Scn1a mutants. **B.** The efficacy of memantine (10 mg/kg i.p.) pretreatment (30-60 minutes before hyperthermic seizure), **C.** post-treatment (6 and 12 hours after hyperthermic seizure), and **D.** combined pre-/post-treatment were analyzed. The duration of treatment is shown in the yellow shade, and the duration of the post-hyperthermic seizure period is in the pink shade. At right, the frequency of total events was increased in control (**A**) pre-treatment (**B**), and post-treatment (**C**), while the combined pre-/post-treatment (**D**) prevented upregulation of events. Statistics were calculated by paired *t*-test.

Interictal and postictal motor behaviors associated with SD

We next analyzed mouse motor behaviors associated with SD using electromyography (EMG) electrodes implanted in the neck muscle. The analysis revealed stereotypical motor behavior patterns accompanying interictal SD, characterized by a prodromal activity increase prior to SD detection with the parietal electrode, followed by suppression of voluntary motor activity for minutes after SD was detected over the frontal cortex (**Figure 5A**). In contrast, seizures are associated with a robust EMG signal increase upon onset (**Figure 5B**). In some mice, such convulsive EMG signals were transiently suppressed when PGES is present (data not shown). Subsequently, the mice showed bursts of motor activities resulting in postictal motor behavior activation lasting for minutes. In a seizure+SD complex, the initial seizure also triggered a sharp EMG activity burst, followed by a transient reduction when SD is detected by the frontal electrode (**Figure 5C**). In the majority of mice, the EMG activity is sustained low after SD except for some burst activities seen in some mice. Overall, seizure+SD showed a lower motor behavior activity compared with seizure ($p<0.001$, analysis of variance of aligned rank transformed data). Overall these results suggest a significant motor behavior suppression effect of spontaneous SDs in the Scn1a$^{+/RX}$ mice.

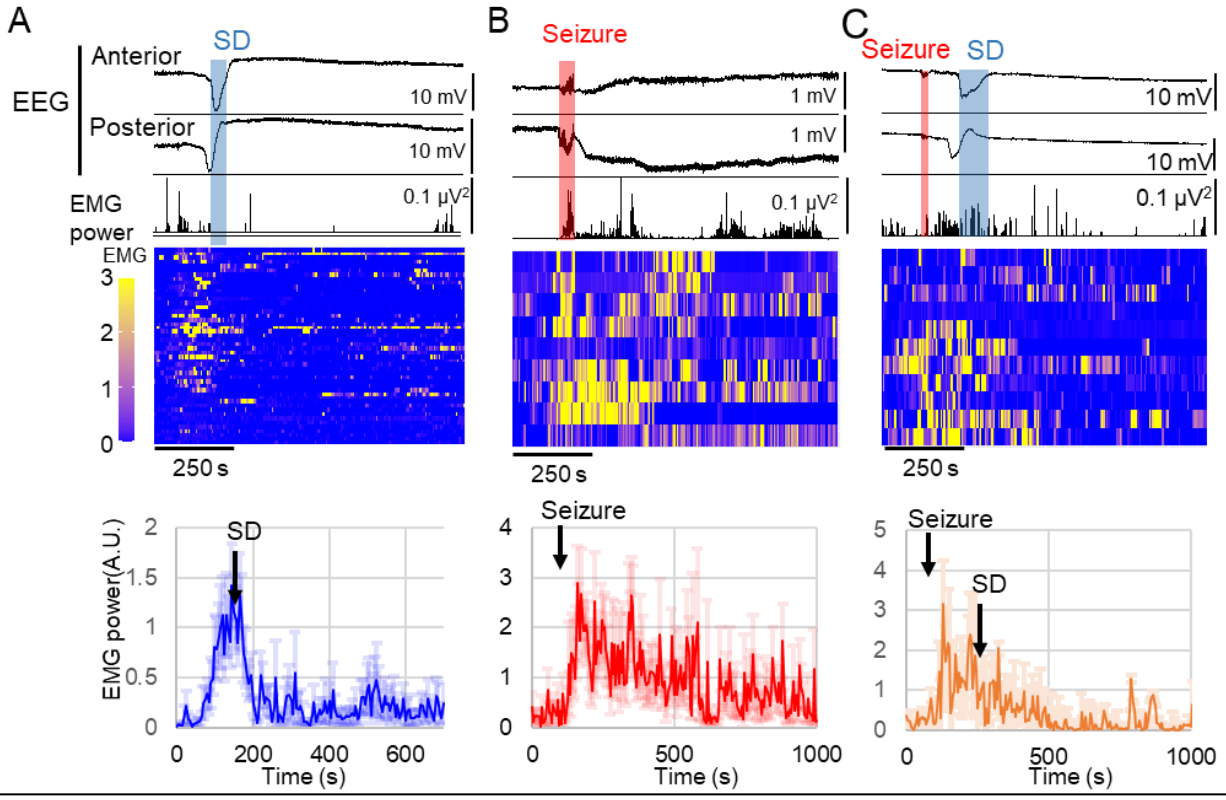

Figure 5. EMG analysis of motor behavior associated with SD (**A**), seizure (**B**), and seizure+SD (**C**). Top EEG and EMG trace. Middle raster plot of individual analyzed EMG signal patterns. The bottom averaged traces of EMG activity are presented as mean ± standard error. Each lane represents a single event. **A.** SD was associated with prodromal behavior activation, followed by suppression as DC shift is detected in the frontal cortex. **B.** Seizure is associated with an abrupt increase in EMG signal which is followed by multiple motor activations. **C.** Seizure+SD is also associated with initial convulsion, while it is inhibited when SD is detected with the frontal cortex. Motor activities are present after SD but are reduced compared with seizure alone. n= 47, 9, and 11 events for SD, seizure, and seizure+SD, respectively.

Locomotion activity concomitant with seizure, SD, and seizure+SD

Lastly, we analyzed the locomotion activity surrounding seizure, SD, and seizure+SD events by video image analysis. In total, 38 seizures, 72 SDs, and 14 seizure+SD from 7 mice were analyzed after the removal of low-quality images. Locomotion during 5-second bins was averaged and binarily determined as active or inactive based on the presence or absence of movement. This analysis detected that the locomotion activities prior to and after seizure+SD were significantly lower than activities surrounding seizure alone (**Figure 6A&B**). A comparison of individual events revealed that seizure+SD tends to reduce locomotion activity from the baseline level (p=0.052, n=14, paired t-test), and the effect becomes significant when nine events without baseline activity were excluded from analysis (p<0.029, n=5, paired t-test). Seizure and SD did not show consistent directional changes in post-locomotion activity.

Together, the motor behavior analysis highlights striking differences in the seizure and seizure+SD complex. The distinct prodromal motor behaviors again suggests isolated seizure and seizure+SD complex are regulated independently likely by the neurophysiological status before seizure onset.

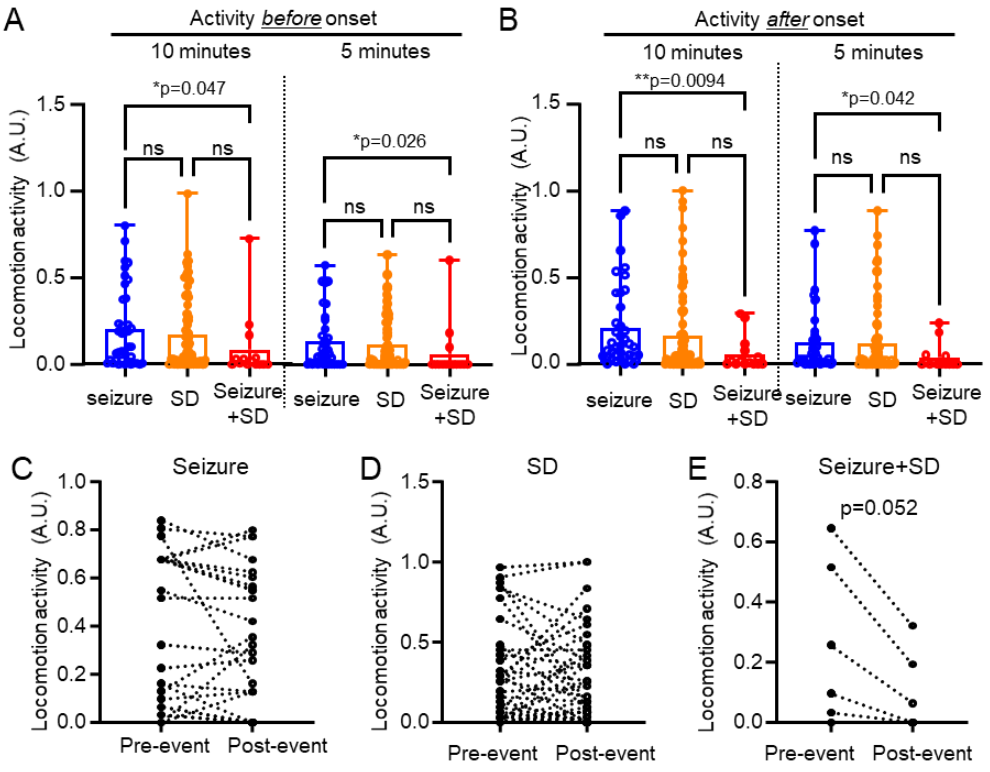

Figure 6. Locomotion activity changes associated with seizure, SD, and seizure+SD. **A&B.** comparison of locomotion activity 10 minutes before (**A**) and after each event (**B**). Seizure+SD is associated with reduced pre- and post-event locomotion activity. Statistics were computed with the Kruskal-Wallis test. **C-E.** Comparing the locomotion activity changes in individual events 3 minutes before and after each event. Seizure and SD did not show consistent directional changes, while seizure+SD consistently reduced the locomotion activity.

Discussion

In this study, we identified a novel spontaneous SD generation phenotype in the Scn1a deficient mouse. SD was frequently detected in Scn1a deficient mice, usually more frequently than seizures, and the incidence of SD is robustly increased after a single hyperthermic seizure, an effect that can last for days or a week. The post-hyperthermia week-long flurry of SD events could be inhibited by memantine only when given before and after the hyperthermic seizure, suggesting that prolonged NMDAR activation contributes to the SD exacerbation. Our electrophysiological and behavioral characterization also revealed that seizures and seizure+SD complexes are qualitatively different and associated with distinct prodromal and postictal behavioral states. These short-term effects may herald more consequential behavioral deficits. Further comparisons and alternative means of pharmacological SD blockade may determine whether identification and management of SD will prove useful for predicting the emergence of subsequent seizure comorbidities. While our preclinical study suggests SD as a prominent pathological event associated with Scn1a deficiency, the overall clinical incidence and significance of SD in epilepsy remain highly limited due to the difficulty of reliably detecting SD in chronic EEG scalp recordings.

Spontaneous cortical SD characteristics of Scn1a deficient mouse

Our study revealed a frequent spontaneous SD in the Scn1a deficient mouse cortex. Correlatively we also observed high SD susceptibility during a hyperthermic seizure in the Scn1a deficient mouse cortex. A similar SD generation after a heat-induced seizure was documented in a recentCa^{2+} imaging study [24]. Clinically, high brain temperature facilitates SD generation [25]. This underscores the higher SD susceptibility of Scn1a deficient brain, since SD during hyperthermic seizure was more common in $Scn1a^{+/RX}$ mice despite the fact that their seizures were provoked at a lower body temperature than WT.

In our recordings, more than 97% of spontaneous SD events were detected sequentially from the posterior to anterior electrodes, suggesting preferential SD generation in the posterior occipital cortex. This is somewhat inconsistent with the high anatomical SD susceptibility in the somatosensory barrel cortex described in the rodent [26,27] which is located closer to the anterior electrodes. This discrepancy might indicate that spontaneous SD generation in $Scn1a^{+/RX}$ mice differs from commonly studied SD models. In a model of type-2 familial hemiplegic migraine, spontaneous SD arises as a consequence of localized glutamate deregulation associated with genetically impaired astrocytes [28]. Such a mechanism is unlikely to explain the SD susceptibility of the sodium channel deficient mouse studied here. Instead, our results predict localized circuit defects in the posterior occipital visual cortex. Along this line, DS patients often report photosensitivity as a comorbidity [29] and the Scn1a deficient mouse has behavioral photosensitivity [30]. A cortical microcircuit-based study of this mouse model may help identify an SD hotspot and understand the SD generation mechanism.

We also identified unique properties of seizure+SD complexes in the Scn1a deficient mouse. The duration of seizure in seizure+SD was shorter than those in isolated events. Together with the lower prodromal locomotion activity in seizure+SD than during isolated seizures, the emergence of postictal SD may be somehow pre-determined by prodromal physiological status. We also found that the duration of SD in seizure+SD was shorter than for an isolated SD. This was somewhat unexpected as we expected seizures would deplete intracellular ATP stores and prolong the depolarization. While an exact reason remains to be elucidated, the effect may be explained by adaptive changes in ion channel/transporter expression and cerebral blood flow regulation. We also detected a stereotyped delay in postictal SD onset, almost always one minute after seizure termination. This is in contrast to the Kcnq2 conditional KO mouse in which most SDs were generated even before seizure

activity fully terminated [7]. This result highlights the distinct SD regulatory mechanisms between epilepsy models with specific circuit defects.

Aggravation of SD phenotype by a hyperthermic seizure

Febrile seizure due to infection or prolonged heat exposure is a common pathogenic mechanism of DS. Similar disease exacerbating effects of hyperthermic seizures were reported in juvenile developing mice [31]. Our observation is generally consistent with these earlier studies and further extended by demonstrating that 1) a single brief seizure is sufficient to provoke an upsurge of SD, 2) exacerbation can occur in adult mice older than P100, and 3) the hyperthermic seizure effect is prevented by concomitant memantine administration. This evidence suggests that disease progression by a febrile seizure can occur independent of developmental stages, and that the exacerbation of phenotype is not solely a developmental defect, but likely involves a proexcitatory plasticity mechanism. This is consistent with studies demonstrating that postnatal Scn1a deletion can create an epileptic encephalopathy similar to the genomic model [32,33], and also that the disease phenotype can be reversed or ameliorated when Scn1a expression is recovered at a juvenile age [34–36]. These findings suggest a life-long risk of exacerbation of disease to severe epilepsy encephalopathy, but also a potential for reversal of disease if the underlying mechanism can be appropriately targeted.

The demonstration that memantine can inhibit the febrile seizure effect suggests a disease mechanism involving chronic NMDAR activation during and after a febrile seizure which may contribute to the febrile seizure effect. We identified two limitations to the direct clinical translation of this treatment. Maximal suppression was found when memantine was administered before the hyperthermia episode, and an excessive memantine dose had a pro-convulsive effect. The latter is probably related to the paradoxical convulsive or excitatory effect of NMDAR inhibition. For example, acute NMDAR inhibition preferentially inhibits GABAergic interneurons [37], while chronic depletion increases neuronal synaptic and intrinsic excitability [38–41]; furthermore, some loss of function NMDAR mutations are associated with developmental epilepsy [42]. This excitatory effect may be beneficial in Alzheimer's disease, but the effects of long-term memantine use in epileptic encephalopathy are unknown. A better understanding of the underlying cellular and molecular mechanism may identify more appropriate treatment options.

Behavior consequence of spontaneous SD

Our study also revealed that spontaneous SD is associated with motor behavior changes. A characteristic of the interictal SD evoked motor behavior suppression after SD invasion in the frontal cortex is generally consistent with findings from optogenetically evoked SD in WT mice [43]. We consistently detected a prodromal motor activity increase before SD initiation. Such prodromal behavior activation likely reflects the local brain excitation associated with SD generation. A study in an α2-Na/K ATPase conditional KO mouse also described a paralyzing effect of putative cortical SD events [44], however the paralysis status described in that study more closely resembles postictal coma than immobility. Postictal immobility has been linked to the risk of severe respiratory dysfunction and sudden unexpected death in epilepsy (SUDEP) [20]. It will be important to examine whether the presence of postictal SD also modifies the cardiorespiratory consequences of seizure.

In contrast to the acute behavioral effect identified here, the lasting effects of SD on the global neurological disorder remain to be elucidated. Previous studies suggest recurrently provoked SD can create chronic deficits

associated with migraine with aura, such as hyperalgesia, photophobia, and anxiety [4,5]. In the current study design, we could not accurately measure these parameters because such behavior tests interrupt the EEG recording and potentially affect the seizure/SD generation pattern. More controlled behavioral characterizations will be needed to understand the long-term contribution of spontaneous SD to neurological deficits associated with this developmental epileptic encephalopathy.

Conclusion

The present study identified a prominent novel SD phenotype and disturbed motor behavior associated with these depolarizing events in the Scn1a deficient mouse model of Dravet syndrome. Together with our recent study of potassium channel deficient mouse models of DEE, SD may represent a new and significant neurological mechanism underlying the complex neurological deficits associated with genetic epileptic encephalopathy.

References

1. Somjen GG. Mechanisms of spreading depression and hypoxic spreading depression-like depolarization. Physiol. Rev. 2001;81(3):1065–1096.

2. Dreier JP. The role of spreading depression, spreading depolarization and spreading ischemia in neurological disease. Nat. Med. 2011;17(4):439–447.

3. Ayata C. Cortical spreading depression triggers migraine attack: pro. Headache 2010;50(4):725–730.

4. Harriott AM, Chung DY, Uner A, et al. Optogenetic Spreading Depression Elicits Trigeminal Pain and Anxiety Behavior. Ann Neurol 2020;Jan;89(1):99–110.

5. Tang C, Unekawa M, Kitagawa S, et al. Cortical spreading depolarisation-induced facial hyperalgesia, photophobia and hypomotility are ameliorated by sumatriptan and olcegepant. Sci Rep 2020;10(1):11408.

6. Dreier JP, Major S, Pannek H-W, et al. Spreading convulsions, spreading depolarization and epileptogenesis in human cerebral cortex. Brain 2012;135(Pt 1):259–275.

7. Aiba I, Noebels JL. Kcnq2/Kv7.2 controls the threshold and bihemispheric symmetry of cortical spreading depolarization. Brain 2021;144(9):2863–2878.

8. Rogawski MA. Migraine and Epilepsy—Shared Mechanisms within the Family of Episodic Disorders [Internet]. In: Noebels JL, Avoli M, Rogawski MA, et al., editors. Jasper's Basic Mechanisms of the Epilepsies. Bethesda (MD): National Center for Biotechnology Information (US); 2012[cited 2022 Jan 21] Available from: http://www.ncbi.nlm.nih.gov/books/NBK98193/

9. Ogiwara I, Iwasato T, Miyamoto H, et al. Nav1.1 haploinsufficiency in excitatory neurons ameliorates seizure-associated sudden death in a mouse model of Dravet syndrome. Hum Mol Genet 2013;22(23):4784–4804.

10. Yamagata T, Ogiwara I, Tatsukawa T, et al. *Scn1a* -GFP transgenic mouse revealed Nav1.1 expression in neocortical pyramidal tract projection neurons [Internet]. Neuroscience; 2021.[cited 2021 May 24] Available from: http://biorxiv.org/lookup/doi/10.1101/2021.03.31.437794

11. Smith RS, Kenny CJ, Ganesh V, et al. Sodium Channel SCN3A (NaV1.3) Regulation of Human Cerebral Cortical Folding and Oral Motor Development. Neuron 2018;99(5):905-913.e7.

12. Yu FH, Mantegazza M, Westenbroek RE, et al. Reduced sodium current in GABAergic interneurons in a mouse model of severe myoclonic epilepsy in infancy. Nat. Neurosci. 2006;9(9):1142–1149.

13. Ogiwara I, Miyamoto H, Morita N, et al. Nav1.1 localizes to axons of parvalbumin-positive inhibitory interneurons: a circuit basis for epileptic seizures in mice carrying an Scn1a gene mutation. J. Neurosci. 2007;27(22):5903–5914.

14. Auffenberg E, Hedrich UB, Barbieri R, et al. Hyperexcitable interneurons trigger cortical spreading depression in an Scn1a migraine model. J Clin Invest 2021;131(21):e142202.

15. Catterall WA, Kalume F, Oakley JC. NaV1.1 channels and epilepsy. J Physiol 2010;588(Pt 11):1849–1859.

16. Connolly MB. Dravet Syndrome: Diagnosis and Long-Term Course. Can. J. Neurol. Sci. 2016;43(S3):S3–S8.

17. Wobbrock JO, Findlater L, Gergle D, Higgins JJ. The aligned rank transform for nonparametric factorial analyses using only anova procedures [Internet]. In: Proceedings of the SIGCHI Conference on Human Factors in Computing Systems. Vancouver BC Canada: ACM; 2011 p. 143–146.[cited 2022 Sep 10] Available from: https://dl.acm.org/doi/10.1145/1978942.1978963

18. Teran FA, Kim Y, Crotts MS, et al. Time of Day and a Ketogenic Diet Influence Susceptibility to SUDEP in Scn1a R1407X/+ Mice. Front Neurol 2019;10:278.

19. Oakley JC, Kalume F, Yu FH, et al. Temperature- and age-dependent seizures in a mouse model of severe myoclonic epilepsy in infancy. Proc Natl Acad Sci U S A 2009;106(10):3994–3999.

20. Kuo J, Zhao W, Li C-S, et al. Postictal immobility and generalized EEG suppression are associated with the severity of respiratory dysfunction. Epilepsia 2016;57(3):412–417.

21. Morimoto T, Kida K, Nagao H, et al. The pathogenic role of the NMDA receptor in hyperthermia-induced seizures in developing rats. Brain Res Dev Brain Res 1995;84(2):204–207.

22. Beconi MG, Howland D, Park L, et al. Pharmacokinetics of memantine in rats and mice. PLoS Curr 2011;3:RRN1291.

23. Creeley C, Wozniak DF, Labruyere J, et al. Low doses of memantine disrupt memory in adult rats. J. Neurosci. 2006;26(15):3923–3932.

24. Tran CH, Vaiana M, Nakuci J, et al. Interneuron Desynchronization Precedes Seizures in a Mouse Model of Dravet Syndrome. J Neurosci 2020;40(13):2764–2775.

25. Schiefecker AJ, Kofler M, Gaasch M, et al. Brain temperature but not core temperature increases during spreading depolarizations in patients with spontaneous intracerebral hemorrhage. J Cereb Blood Flow Metab 2018;38(3):549–558.

26. Bogdanov VB, Middleton NA, Theriot JJ, et al. Susceptibility of Primary Sensory Cortex to Spreading Depolarizations. J Neurosci 2016;36(17):4733–4743.

27. Juzekaeva E, Nasretdinov A, Gainutdinov A, et al. Preferential Initiation and Spread of Anoxic Depolarization in Layer 4 of Rat Barrel Cortex. Front Cell Neurosci 2017;11:390.

28. Parker PD, Suryavanshi P, Melone M, et al. Non-canonical glutamate signaling in a genetic model of migraine with aura. Neuron 2021;109(4):611-628.e8.

29. Verbeek N, Kasteleijn-Nolst Trenité D, Wassenaar M, et al. Photosensitivity in Dravet syndrome is under-recognized and related to prognosis. Clin Neurophysiol 2017;128(2):323–330.

30. Han S, Yu FH, Schwartz MD, et al. Na(V)1.1 channels are critical for intercellular communication in the suprachiasmatic nucleus and for normal circadian rhythms. Proc Natl Acad Sci U S A 2012;109(6):E368-377.

31. Salgueiro-Pereira AR, Duprat F, Pousinha PA, et al. A two-hit story: Seizures and genetic mutation interaction sets phenotype severity in SCN1A epilepsies. Neurobiology of Disease 2019;125:31–44.

32. Stein RE, Kaplan JS, Li J, Catterall WA. Hippocampal deletion of Na_V 1.1 channels in mice causes thermal seizures and cognitive deficit characteristic of Dravet Syndrome. Proc. Natl. Acad. Sci. U.S.A. 2019;116(33):16571–16576.

33. Jansen NA, Dehghani A, Breukel C, et al. Focal and generalized seizure activity after local hippocampal or cortical ablation of NaV 1.1 channels in mice. Epilepsia 2020;61(4):e30–e36.

34. Yamagata T, Raveau M, Kobayashi K, et al. CRISPR/dCas9-based Scn1a gene activation in inhibitory neurons ameliorates epileptic and behavioral phenotypes of Dravet syndrome model mice. Neurobiology of Disease 2020;141:104954.

35. Tanenhaus A, Stowe T, Young A, et al. Cell-Selective Adeno-Associated Virus-Mediated *SCN1A* Gene Regulation Therapy Rescues Mortality and Seizure Phenotypes in a Dravet Syndrome Mouse Model and Is Well Tolerated in Nonhuman Primates. Human Gene Therapy 2022;33(11–12):579–597.

36. Valassina N, Brusco S, Salamone A, et al. Scn1a gene reactivation after symptom onset rescues pathological phenotypes in a mouse model of Dravet syndrome. Nat Commun 2022;13(1):161.

37. Homayoun H, Moghaddam B. NMDA receptor hypofunction produces opposite effects on prefrontal cortex interneurons and pyramidal neurons. J. Neurosci. 2007;27(43):11496–11500.

38. Lüthi A, Schwyzer L, Mateos JM, et al. NMDA receptor activation limits the number of synaptic connections during hippocampal development. Nat Neurosci 2001;4(11):1102–1107.

39. Fukushima F, Nakao K, Shinoe T, et al. Ablation of NMDA Receptors Enhances the Excitability of Hippocampal CA3 Neurons. PLoS ONE 2009;4(1):e3993.

40. Tatard-Leitman VM, Jutzeler CR, Suh J, et al. Pyramidal cell selective ablation of N-methyl-D-aspartate receptor 1 causes increase in cellular and network excitability. Biol Psychiatry 2015;77(6):556–568.

41. Hou G, Zhang Z-W. NMDA Receptors Regulate the Development of Neuronal Intrinsic Excitability through Cell-Autonomous Mechanisms. Front Cell Neurosci 2017;11:353.

42. XiangWei W, Jiang Y, Yuan H. De Novo Mutations and Rare Variants Occurring in NMDA Receptors. Curr Opin Physiol 2018;2:27–35.

43. Houben T, Loonen IC, Baca SM, et al. Optogenetic induction of cortical spreading depression in anesthetized and freely behaving mice. J Cereb Blood Flow Metab 2017;37(5):1641–1655.

44. Smith SE, Chen X, Brier LM, et al. Astrocyte deletion of α2-Na/K ATPase triggers episodic motor paralysis in mice via a metabolic pathway. Nat Commun 2020;11(1):6164.